

Corrosion products formed during corrosion of stainless steel in concrete

M. Serdara, C. Meral, M. Kunz, Dubravka Bjegovica, Hans-Rudolf Wenk , P.J.M. Monteiro, Spatial distribution of crystalline corrosion products formed during corrosion of stainless steel in concrete, Cement and Concrete Research, volume: **71** page: **93 -105**.

Stainless Steels

Nowadays, stainless steels are widely utilized as reinforcement instead of carbon steel, especially when durability due to aggressive environment exposure is a concern.

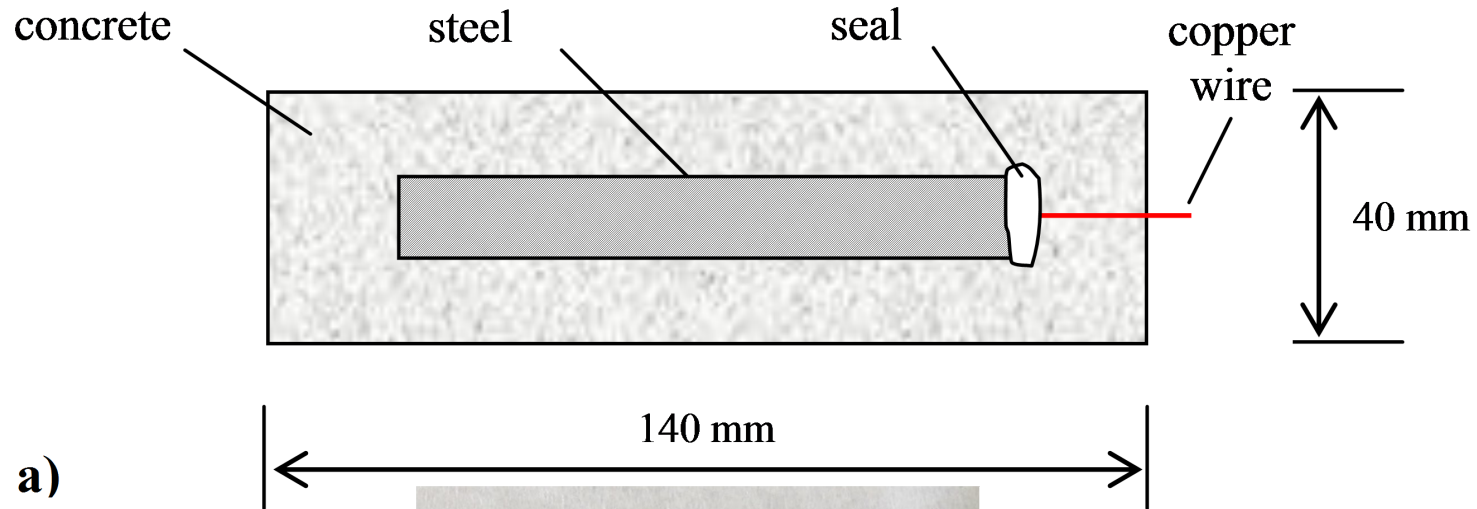
Stainless Steels

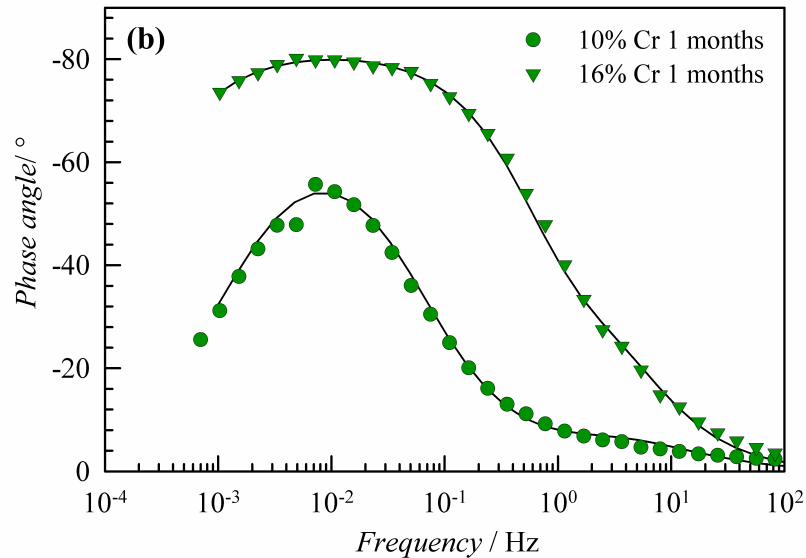
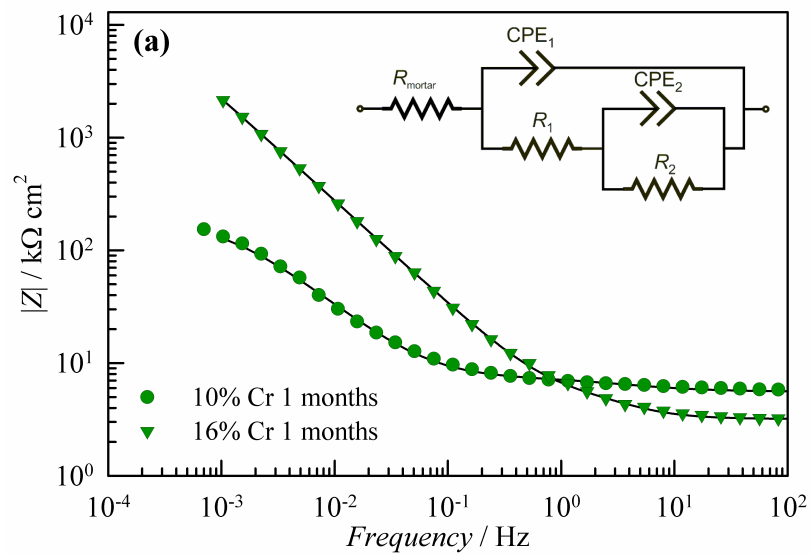
Because of rising nickel prices, new types of corrosion resistant steels with lower percentages of alloying elements have been developed, e.g., low-nickel, high-chromium corrosion-resistant steels, which can be a cost-effective corrosion resistant alternative to highly alloyed stainless steels

Elemental composition of the steels

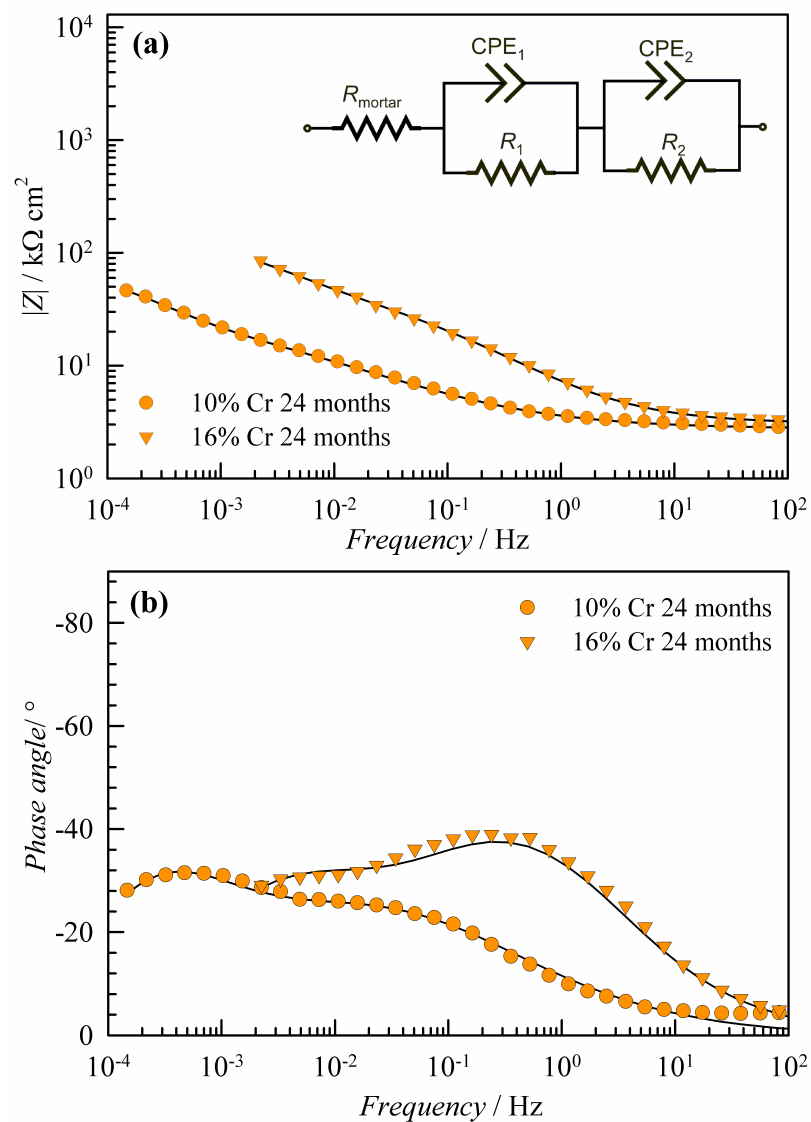
Steel type	Elemental composition, wt.%									
	C	Si	Mn	S	N	Cr	Cu	Mo	Ni	Fe
10% Cr steel	≤0.03	≤1.00	≤1.50	≤0.015	≤0.03	10.50	-	-	0.30	Bal.
16% Cr steel	≤0.10	≤2.00	7.50	≤0.003	0.15	16.00	2.00	≤1.00	<2.00	Bal.

Samples used

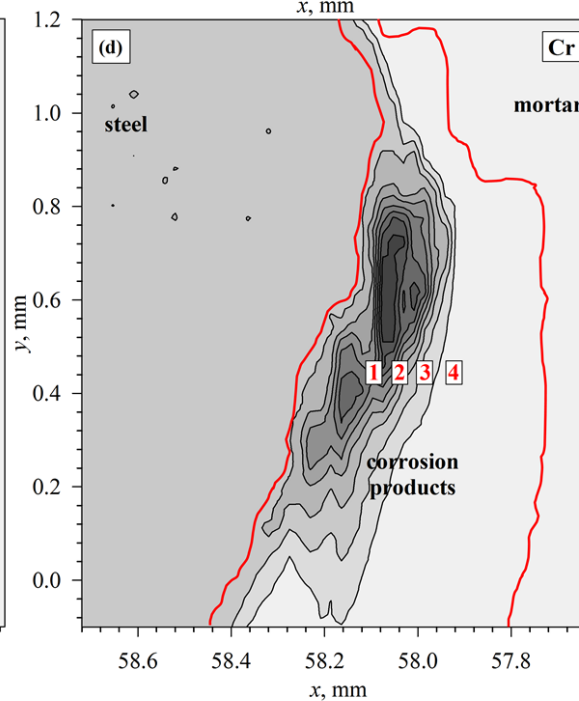
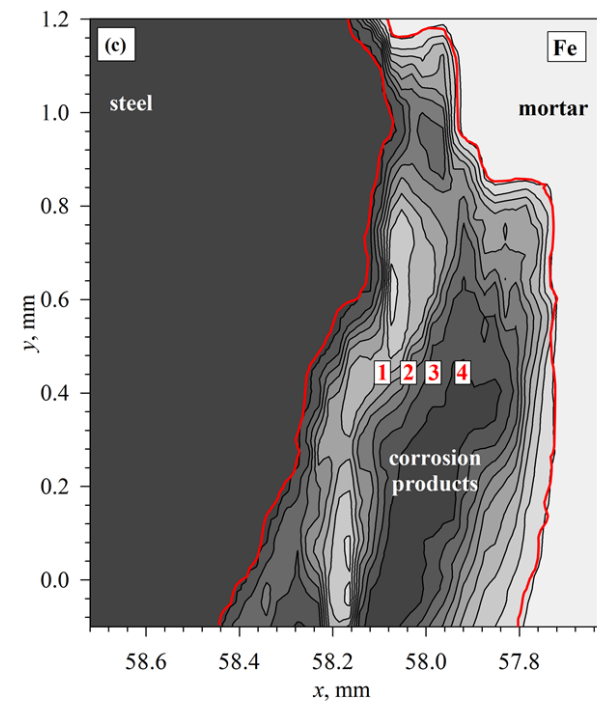
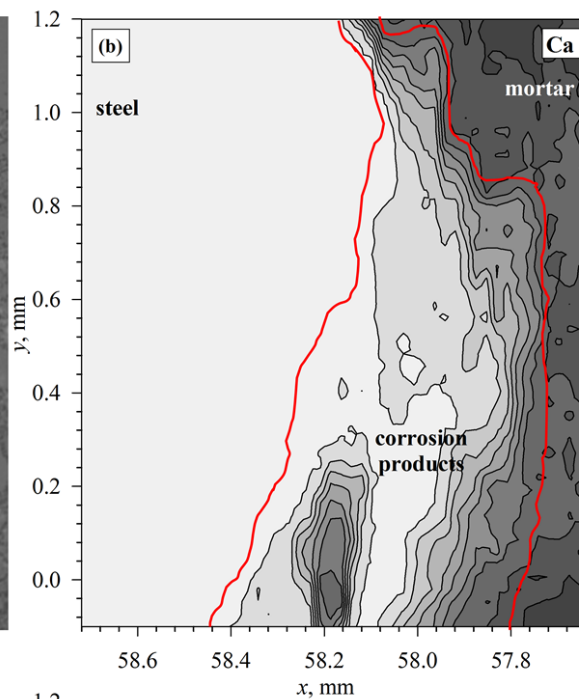
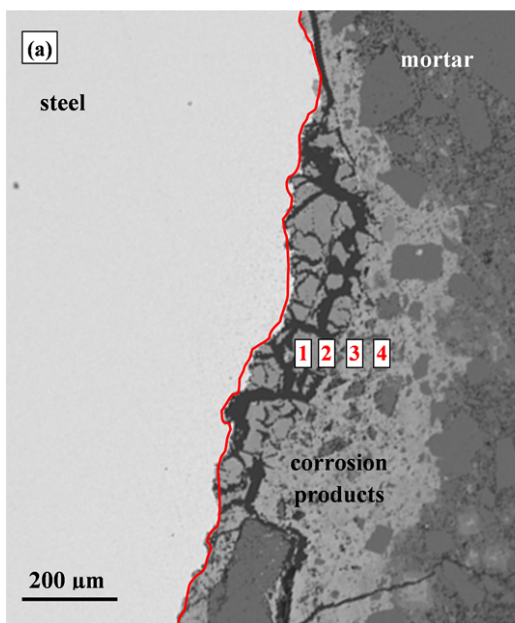




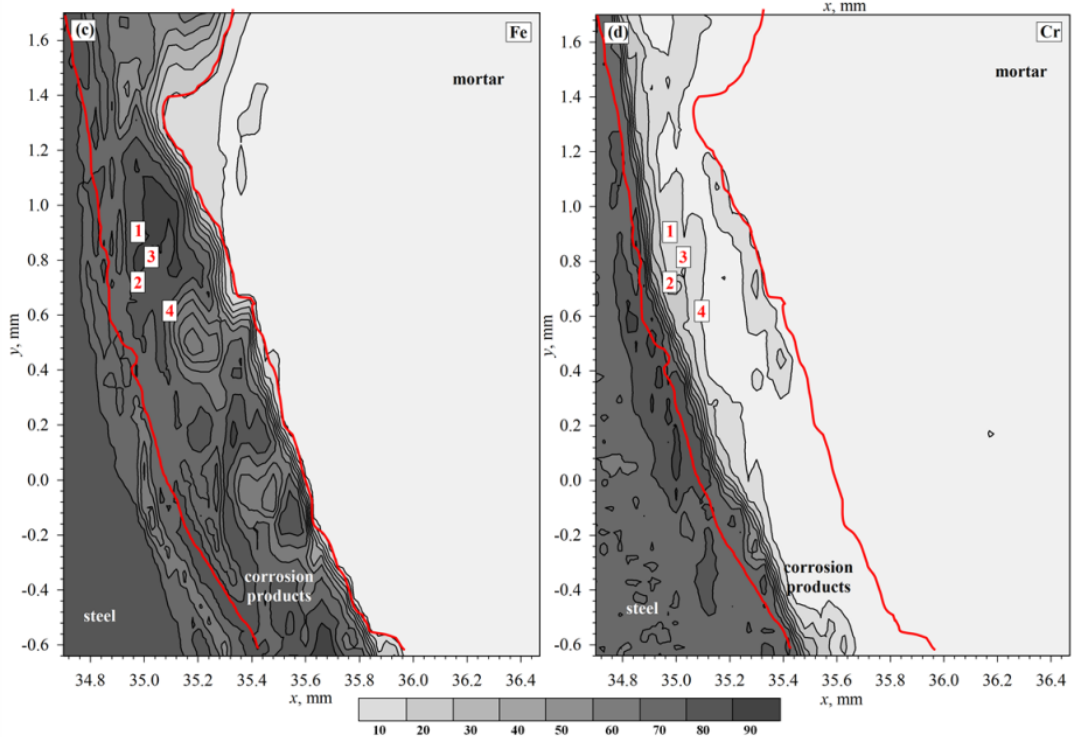
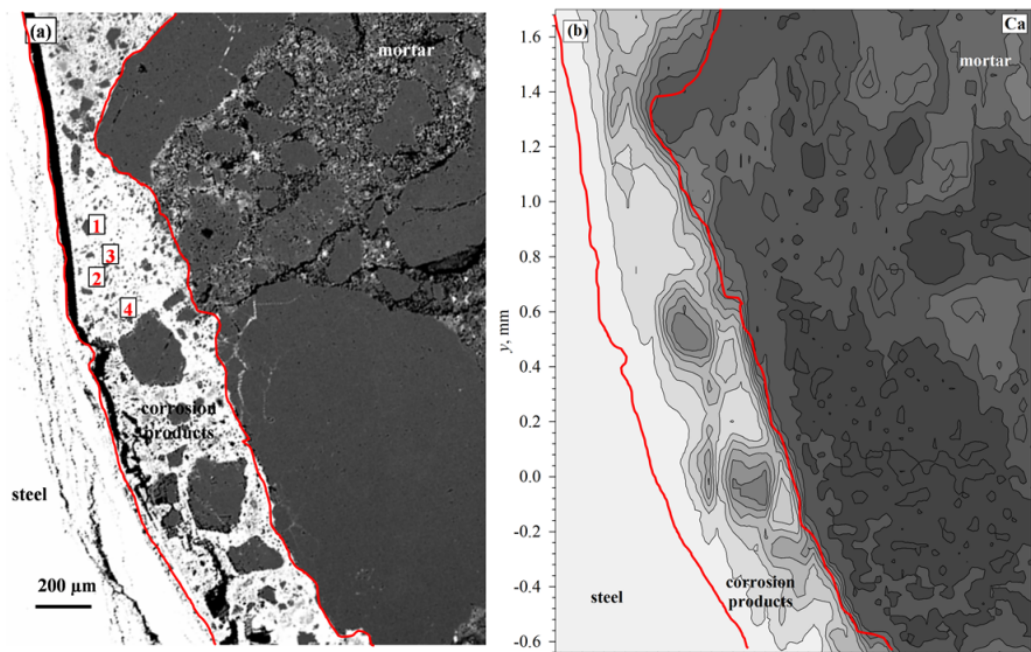
Impedance Spectra for concrete sample reinforced with the 10 wt.% Cr steel and the 16 wt.% Cr steel after 1 month of exposure to 3.5 wt.% NaCl solution



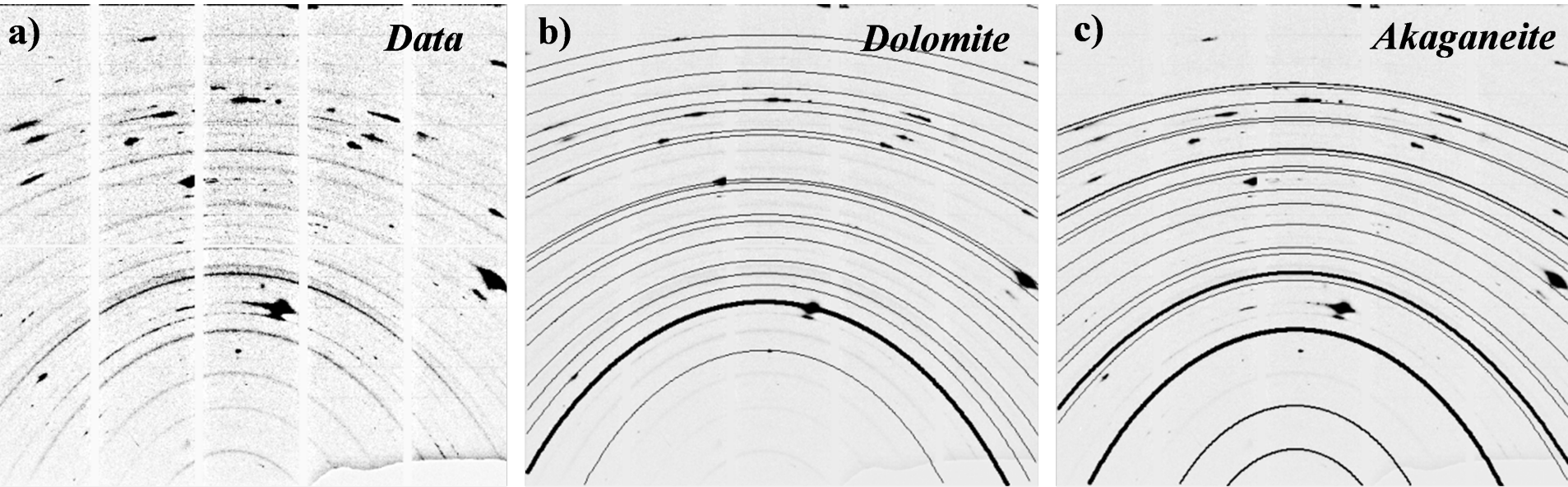
(a) Bode and (b) Nyquist plots of impedance spectra for concrete sample reinforced with the 10 wt.% Cr steel and the 16 wt.% Cr steel after 24 months of exposure to 3.5 wt.% NaCl solution.



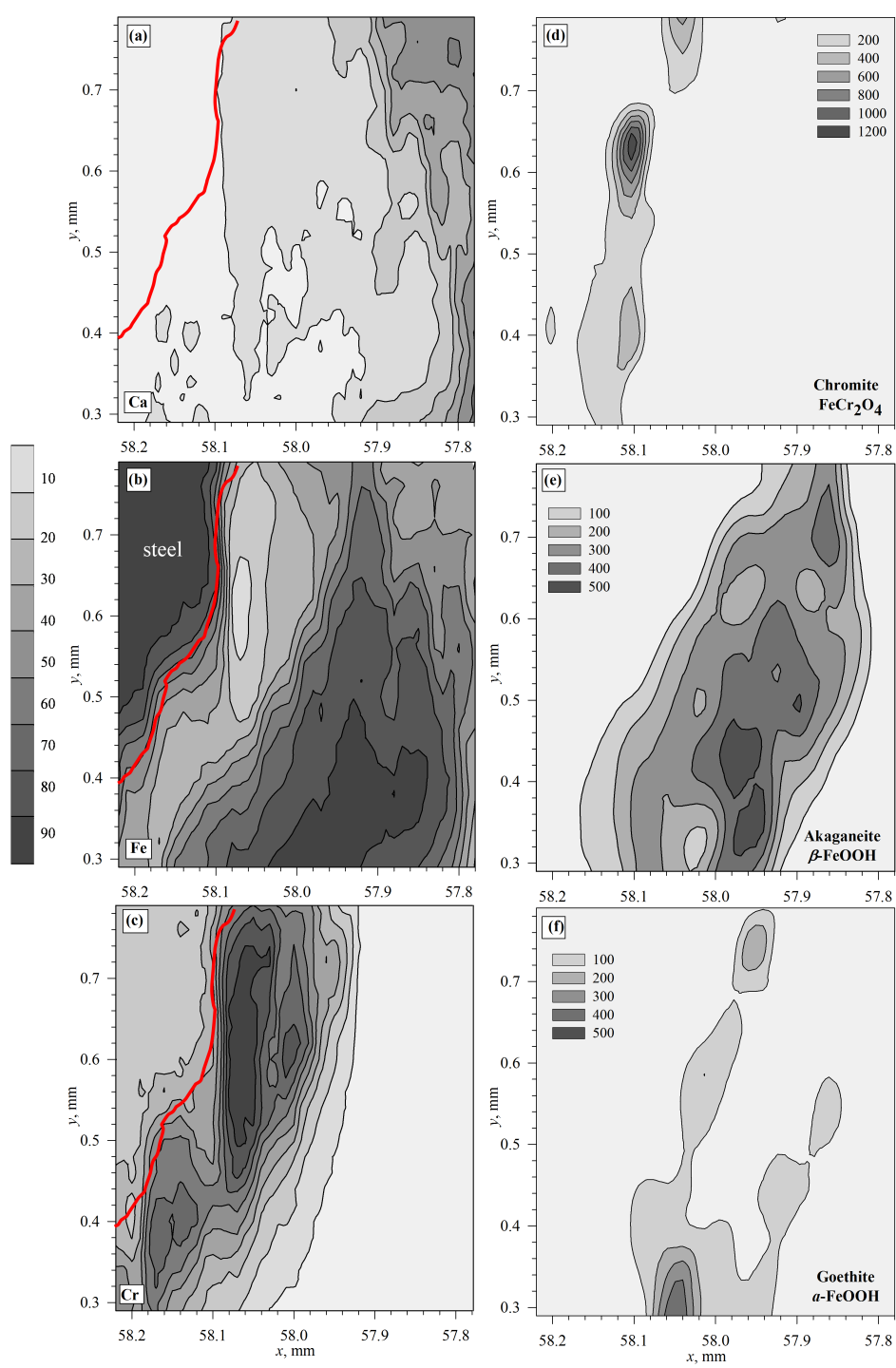
(a) BSE image of the 10wt.% Cr steel and mortar interface; and μ -XRF maps of the same area showing distributions and intensities of (b) calcium, (c) iron and (d) chromium.



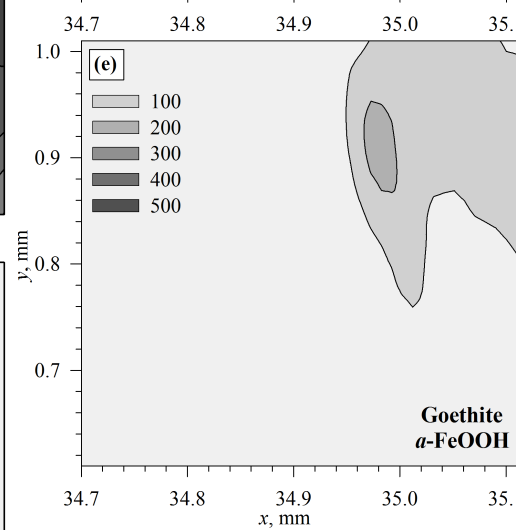
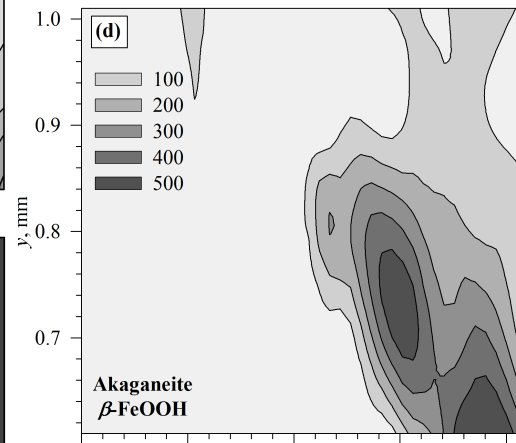
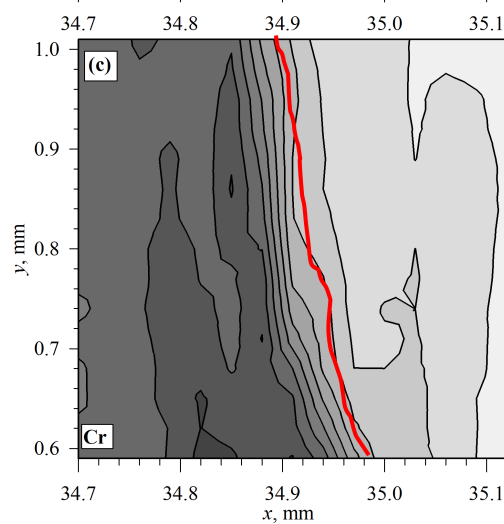
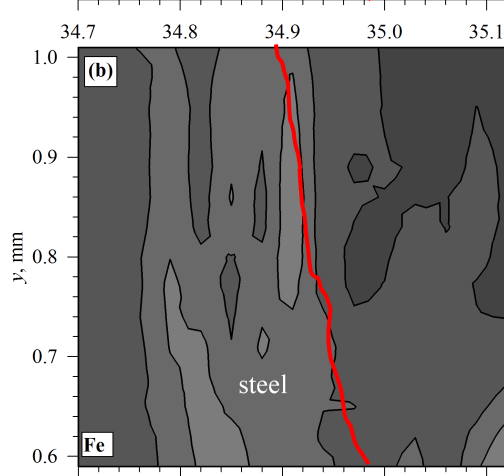
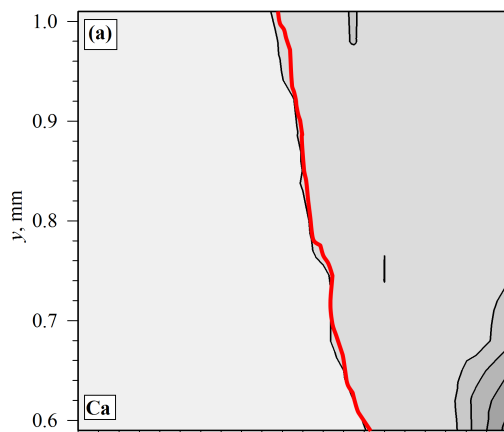
(a) BSE image of the 16wt.% Cr steel and mortar interface; and μ-XRF maps of the same area showing distributions and intensities of (b) calcium, (c) iron and (d) chromium.



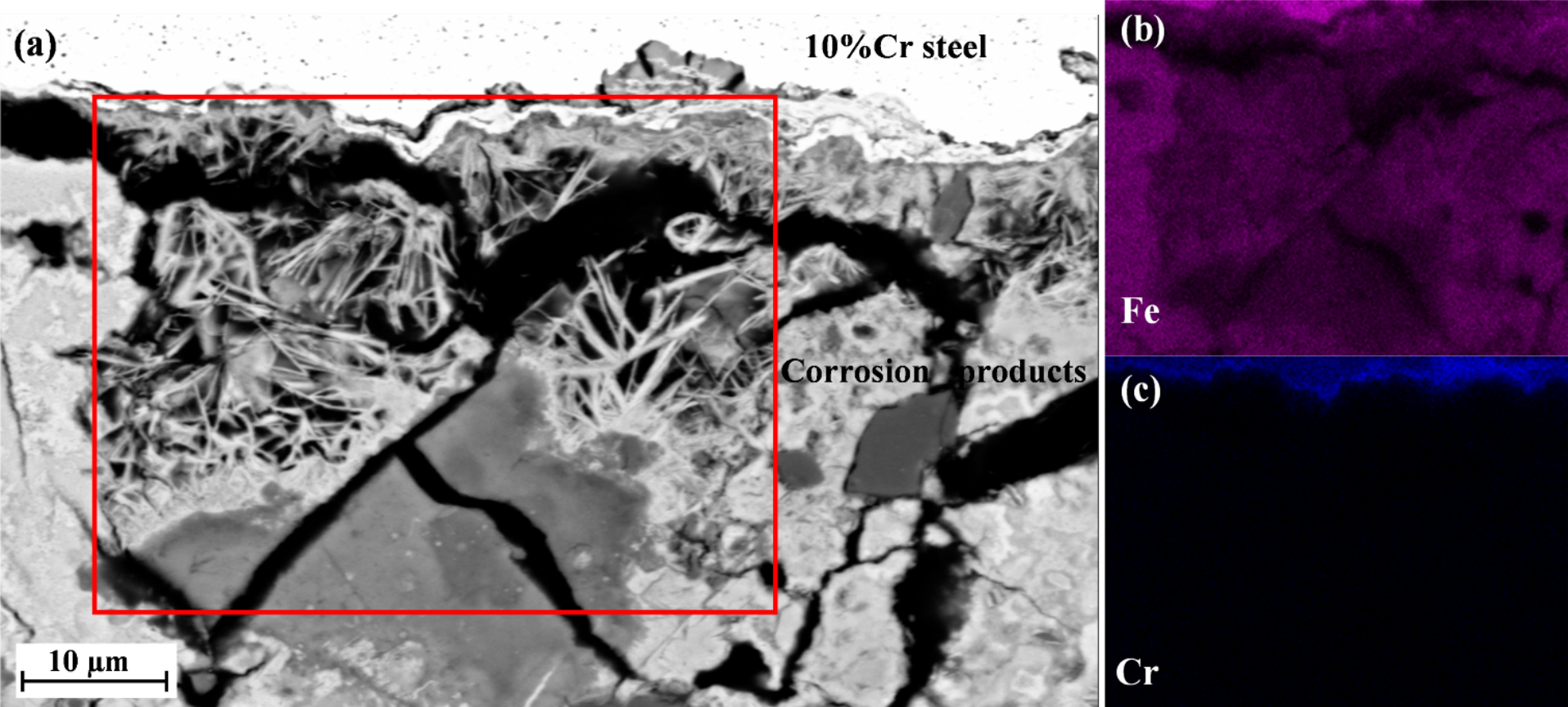
(a) A representative monochromatic μ -XRD pattern (energy= 10 keV) showing partial Debye–Scherrer rings, (b) reflections of dolomite, and (c) reflections of akaganeite



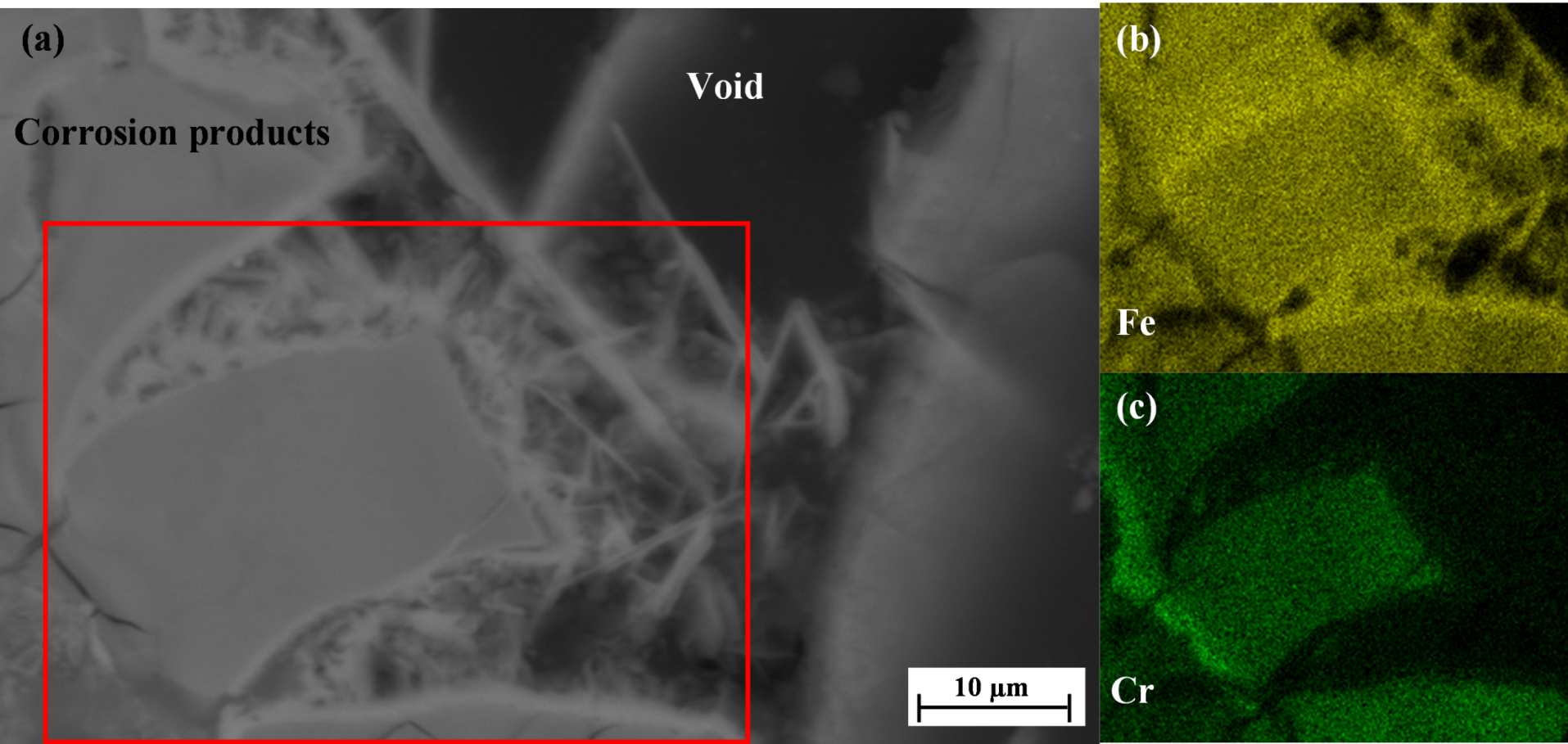
10 wt.% Cr steel reinforced mortar sample: μ -XRF elemental maps for (a) Ca, (b) Fe, and (c) Cr and corresponding intensity maps obtained through μ -XRD measurement showing distribution of (d) chromite (FeCr_2O_4), (e) akaganeite ($\beta\text{-FeOOH}$), and (f) goethite ($\alpha\text{-FeOOH}$).



16 wt.% Cr steel reinforced mortar sample: μ -XRF elemental maps for (a) Ca, (b) Fe, and (c) Cr and corresponding intensity maps obtained through μ -XRD measurement showing distribution of (d) akaganeite (β -FeOOH), and (e) goethite (α -FeOOH).



An example of needle-like crystals mainly formed in voids and cracks around the surface of the 10wt.% Cr steel, BSE image (a) with Fe (b) and Cr (c) distribution maps of the area indicated in the red box on (a), obtained by EDS.



An example of crystals mainly formed in voids in the cement matrix around the 16wt.% Cr steel, BSE image (a) with Fe (b) and Cr (c) distribution maps of the area indicated in the red box on (a), obtained by EDS.

Summary

- Analysis of powder diffraction patterns revealed that the main phases formed during corrosion of two types of high-Cr, low-Ni corrosion resistant steels embedded in mortar were goethite and akageneite.

Summary

- Goethite is predominantly found closer to the surface of the steel and its growth is enhanced by the presence of chromium in the composition of reinforcing steel.

Summary

- Akageneite is found further away from the surface of the steel and its growth is attributed to the presence of chloride ions in the environment around the steel.

Summary

- In the case of steel with higher Cr content, corrosion products with Cr were identified using SEM and EDS.